Conference Proceedings Paper

Hi-Fi Stake Single Crystal Actuators and New Developments

Fang-Chih LIM [1*], Dian-Hua LIN [1], Yuexue XIA [1], Jiahao KOH [1] and Leong-Chew LIM [1]

Published: 3 Nov 2020
Academic Editor:

[1] Microfine Materials Technologies Pte Ltd, 10 Bukit Batok Crescent, #06-02 The Spire, Singapore 658079, SINGAPORE; http://www.microfine-piezo.com
* Correspondence: albertlim@microfine-piezo.com; Tel.: +65 96102365

Abstract: "Hi-Fi Stake" piezoelectric actuators are constructed by bonding [011]-poled d_{32}-mode lead-based relaxor-PT single crystals with polycarbonate edge guides into a square-pipe structure. They contract under positive-polarity applied voltage due to d_{32} values being negative for [011]-poled relaxor-PT single crystals. Under quasi-static loading conditions, Hi-Fi Stake single crystal actuators exhibit highly linear displacement response with negligible hysteresis. Over the years, we have successfully developed the following three versions of Hi-Fi Stake (HFS) actuators: cost-effective (CE), large-stroke (LS) and high-load (HL), all of maximum use temperature up to 60 °C. Of which, the LS version, of 2-level construction, displays strokes of up to 50 μm @ 240 V and the HL version, of 2-layer construction, has maximum loads allowed of 14 kg-f at room temperature and 7 kg-f at 60 °C. Also described in this work are the developments of Cryogenic Hi-Fi Stakes (CG-HFS) and High-Temperature Hi-Fi Stake (HT-HFS) actuators. The selection of suitable crystal compositions, recommended working conditions and measured performance of fabricated prototypes of these two new versions of Hi-Fi Stakes are presented and discussed.

Keywords: linear and hysteresis-free strain; stroke, working load, cryogenic; high temperature

---

1. Introduction

Lead-based relaxor-lead titanate (PT) solid solution single crystals, notably lead zinc niobate-lead titanate ($Pb[Zn_{1/3}Nb_{2/3}]O_3$-$PbTiO_3$ or PZN-PT), lead magnesium niobate-lead titanate ($Pb[Mg_{1/3}Nb_{2/3}]O_3$-$PbTiO_3$ or PMN-PT) and lead indium niobate-lead magnesium nibote-lead titanate ($Pb[In_{1/2}Nb_{1/2}]O_3$-$Pb[Mg_{1/3}Nb_{2/3}]O_3$-$PbTiO_3$ or PIN-PMN-PT), have attracted much attention in the last two decades [1-3]. These single crystals display extraordinarily high piezoelectric coefficients, being 4× to 8× that of lead zirconate titanate (PZT) ceramics. They are thus potential candidate materials for high performance piezoelectric devices.

In addition to their high piezoelectric coefficients, these single crystals display linear strain response with minimum hysteresis especially those of rhombohedral structure having compositions sufficiently away from the morphotropic phase boundary (MPB) [4,5]. Their properties are highly orientation dependent such that while [001]-poled relaxor-PT single crystals exhibit large longitudinal piezoelectric coefficient (d_{33}), [011]-poled relaxor-PT single crystals show exceptional transverse piezoelectric activity when the active direction is also the [100] crystal direction, i.e., they display extremely large d_{32} value which is negative, meaning that a [011]-poled crystal will contract in the [100] crystal direction when a positive polarity voltage is applied to the crystal electrode faces.

There also had been attempts to make multilayer stack actuators out of these single crystals, notably PMN-PT [6,7]. The crystals were first thinned down sufficiently and multiple units of them, up to hundreds in number in certain cases, were then bonded with epoxy into a stack arrangement. However, despite remaining linear, the resultant stack actuators display observable strain hysteresis. One plausible reason for this could be the many layers of single crystal-electrode-epoxy materials within the stacked structure. Since respective layers of material may respond to the electric or mechanical excitation differently, this would lead to undesired local stresses within the structure and hence the strain hysteresis. Besides, fabrication of single crystal stack actuators is a very costly operation because not only the crystal itself is expensive but also the process involved is laborious and time-consuming.

In recent years, we have been experimenting with [011]-poled d_{32}-mode piezo single crystals and fabricate multi-stake actuators out of them. These multi-stake single crystal actuators display highly linear strain behaviour with negligible hysteresis when operated within the rhombohedral phase state [8,9]. In what follows, we shall briefly summrise these findings and present the result of relevant new developments, including cryogenic (CG) and high-temperature (HT) HFS actuators.

2. "Hi-Fi Stake" Single Crystal Actuator

"Hi-Fi Stake" (HFS) piezoelectric single crystal actuators are fabricated by bonding 4 identical rectangular-shaped d_{32}-mode lead-based relaxor-PT single crystals with polycarbonate edge guides into a square-pipe construction and further capped with top and bottom end caps at both ends (see Figure 1a) [8,9]. They offer the following key advantages: (a) improved bending stiffness and strength with minimum crystal volume, (b) unlike transverse-mode single crystal tube structure, all crystals exhibit same axial strain response, (c) minimum number of epoxy joints hence structural-heterogeneity. Both (b) and (c) minimize structural heterogeneities and undesired local stresses and strains within the device during crystal excitation which, together with the linear response of individual single crystals, entail the linear strain response with negligible hysteresis of the resultant device.

Current Hi-Fi stake actuators are made of PZN-PT and/or PIN-PMN-PT d_{32}-mode piezo single crystals. These crystals have reasonably high transformation temperature of 105-125°C and piezoelectric coefficients (see also Fig. 3). This enables the resultant actuators to display reasonably large stroke at low voltages, at up to 60°C with payload. Furthermore, the strain and displacement responses are highly linear with negligible hysteresis.

At present, 3 main types of Hi-Fi Stake (HFS) are available (see Figure 1): (a) cost-effective (CE), (b) large-stroke (LS) and (c) high-load (HL). Cost-effective Hi-Fi Stake (CE-HFS) actuator has the basic square-pipe construction (Fig. 1a). Large-Stroke Hi-Fi Stake (LS-HFS) has a 2-level square-pipe structure (Fig. 1b) for increased device active length, while High-Load Hi-Fi Stake (HL-HFS) has a inner and outer 2- layer square-pipe construction (Fig. 1c) for increased crystal load bearing area.

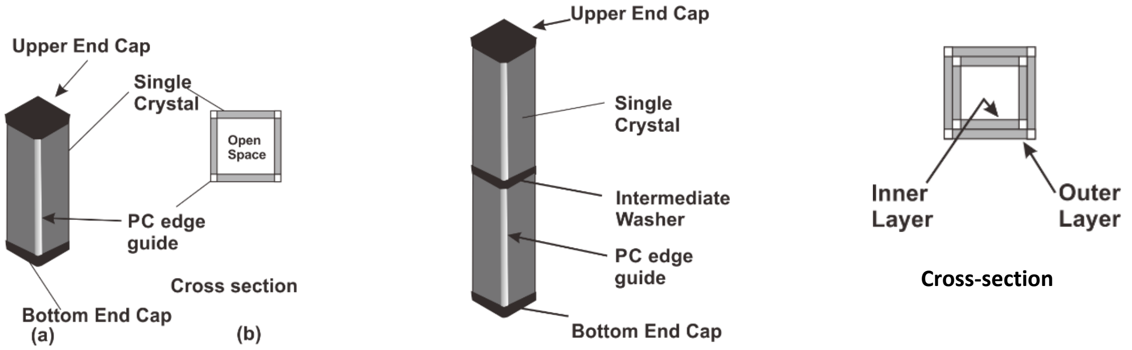

(a) (b) (c)

Figure 1. Constructions of (a) CE-, (b) LS- and (c) HL-HFS single crystal actuators.

Table 1 shows the performance of selected HFS actuators of respective constructions. Figure 2(a) to (c) show the displacement responses of selected HFS actuators. Detailed descriptions of the experimental techniques used for the measurement of displacement, stroke and maximum load allowed can be found in [8,9].

Table 1. Performance of selected Hi-Fi Stake single crystal actuators [10]

Sample No.*	Dimensions $W_1 \times W_2 \times L$ (mm^3)	Stroke @ 240V (μm)	Stiffness (kg-f/μm)	Max. Load Allowed (kg-f)		
				25°C	40°C	60°C
HSF-**CE**-3.6×8L	3.6×3.6×8L	–5	0.35	1.8	1.5	0.9
HSF-**CE**-3.6×15L	3.6×3.6×15L	–12	0.14	1.8	1.5	0.9
HSF-**CE**-5×15L	5×5×15L	–12	0.22	3.0	2.5	1.5
HSF-**CE**-5×28L	5×5×28L	–25	0.10	3.0	2.5	1.5
HSF-**LS**-5×45L	5×5×45L	–41	0.06	3.0	2.5	1.5
HSF-**LS**-5×54L	5×5×54L	–50	0.05	3.0	2.5	1.5
HSF-**LS**-7.5×54L	7.5×7.5×54L	–50	0.08	4.8	4.0	2.4
HSF-**HL**-7.5×15L	7.5×7.5×18L	–12	0.66	8.5	7.5	4.5
HSF-**HL**-10×28L	10×10×28L	–25	0.42	14.0	11.0	7.0

*CE= cost-effective; LS= large-stroke; HL= high-load. Active length L_{ac}= L–3 mm for CE- & HL-HFS; L_{ac}= L–4 mm for LS-HFS.

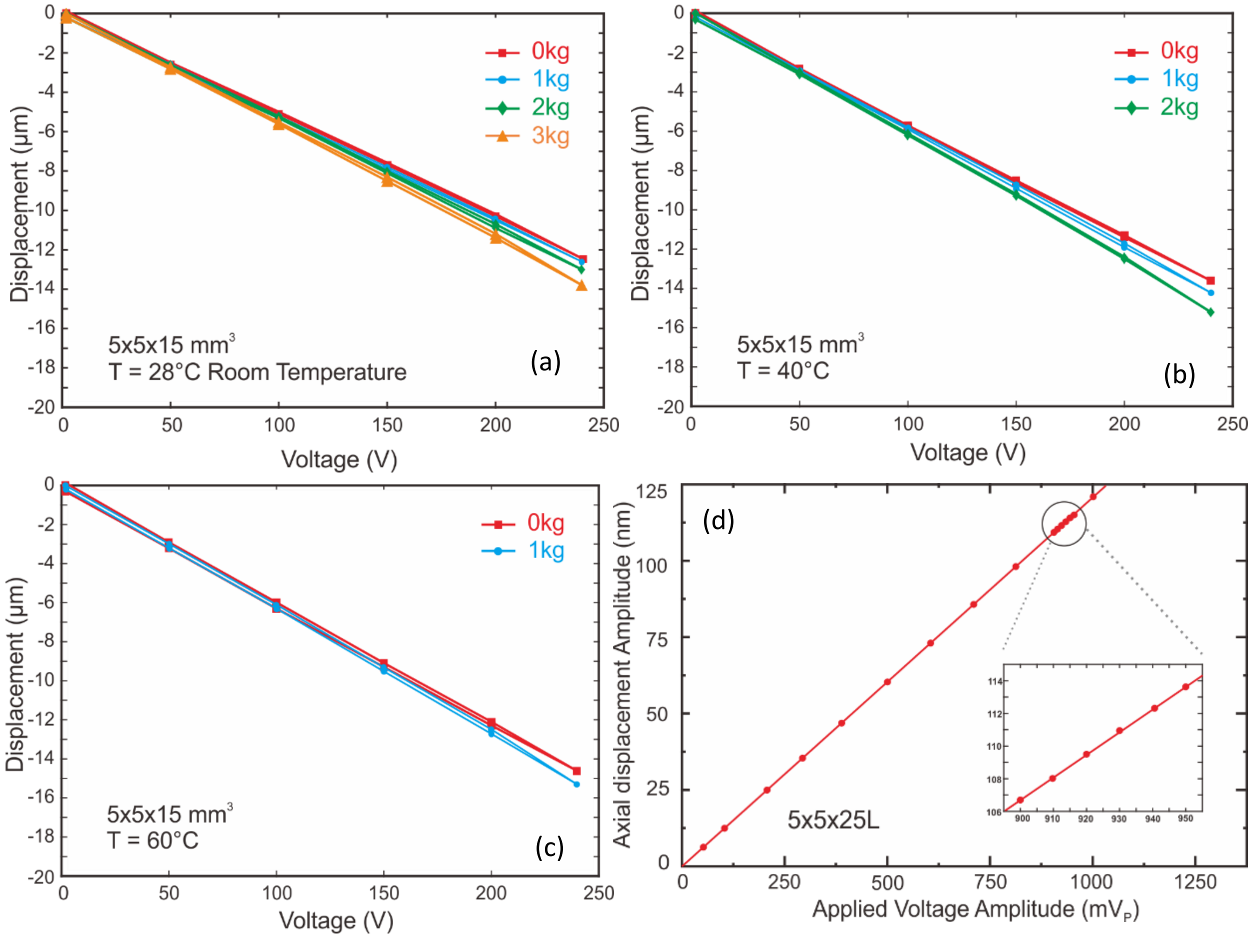

Figure 2. Displacement responses of selected Hi-Fi Stake single crystal actuators at (a) room temperature, (b) 40°C and (c) 60°C. (d) gives the result of vibrometry measurement showing sub-nanometer resolution of a single crystal stake actuator.

These figures show that Hi-Fi Stake single crystal actuators are highly linear with negligible hysteresis when used within the specified conditions. Shown in Figure 2(d) is a displacement curve obtained by laser vibrometry technique using a HFS actuator sample of 5×5×28L mm in dimensions. It shows that the actuator displays 1.5 nm displacement amplitude at 10 mV_P, corresponding to 0.15 nm resolution at 1 mV_P.

In what follows, we shall describe two new developments of Hi-Fi Stake single crystal actuators: Cryogenic Hi-Fi Stake (CG-HFS) and High-Temperature Hi-Fi Stake (HT-HFS).

3. Cryogenic Hi-Fi Stake (CG-HFS) Actuator

Piezoelectric actuators and motors have been deployed in many space applications due to their fast and precision response and free of electromagnetic interference. For such application, the actuators must be compact and light, with adequate stroke and payload, and consume minimum power [11,12]. While piezoelectric actuators made of piezoceramics are widely used, they lose up to 75% of their piezoelectric performance at cryogenic temperatures, severely limiting the strain available [12]. In contrast, recently available lead-based relaxor-PT single crystals not only have several times higher piezoelectric coefficients than present-day piezoceramics but also retain a larger portion of piezoelectric strain at cryogenic temperatures [13,14]. They thus make possible actuators with significantly higher piezoelectric performance both at room and cryogenic temperatures.

In this work, the cryogenic d_{32} values of different relaxor-PT single crystals were studied by the resonance technique using a home-made cryogenic test cell which also allows for concurrent application of electric voltage and axial compressive load to the single crystal and/or actuator samples. Using liquid nitrogen as the cooling medium, the minimum test temperature that the set-up can attain is around −170°C. This temperature is lower than what a space craft will experience when it is completely blocked out of the sunlight by the earth [15].

The following three crystal systems were investigated: PZN-PT and derivatives (including doped and ternary), PIN-PMN-PT and PMN-PT crystals. The results are summarised in Figure 3.

Figure 3 shows that at room temperature, PZN-PT (and its derivatives) and PIN-PMN-PT single crystals exhibit comparable d_{32} and T_{RO} values of 1400-2200 pC/N and 110-125°C. More specifically, within said d_{32} range, the T_{RO} of PIN-PMN-PT crystals are about 3-5°C higher than that of PZN-PT for a given d_{32} value. And, while PZN-PT crystals of higher PT contents (i.e., those of ≥6%PT) display extremely high d_{32} values of ≥2400 pC/N, PIN-PMN-PT crystals of compositions away from the MPB show higher T_{RO} of 125-135°C despite having smaller d_{32} values of 1100-1500 pC/N. PMN-PT single crystals also exhibit comparable d_{32} values at room temperature. They, however, have significantly lower T_{RO} compared with PZN-PT and PIN-PMN-PT.

Typical d_{32} versus temperature curves of representative crystal compositions are provided in Figure 4. This figure shows that over the temperature range from room temperature to −25°C, the d_{32} values decrease steadily for all the three crystal systems. At −50°C, PZN-PT and PIN-PMN-PT crystals retain about 75-80% of their room temperature d_{32} value, while PMN-PT crystal retain about 80-85%.

The rates of decrease in d_{32} value subsize significantly for all the 3 crystal systems over the temperature range from −25°C to −100°C. While the rates of decrease are comparable for both PZN-PT and PIN-PMN-PT crystals with the former showing slightly higher rate, it is a lot more gradual for PMN-PT crystals. As a result, PZN-PT crystals retain about 60%, PIN-PMN-PT about 70% and PMN-PT crystals about 80% of their room temperature d_{32} values at −100°C.

Over the temperature range from −110°C to −170°C, the rates of decrease in d_{32} increase again for all the 3 crystal systems. The rates of decrease are again comparable for PZN-PT and PIN-PMN-PT. In contrast, PMN-PT crystals display a higher decreasing rate over this temperature range. At −150°C the d_{32} values of PZN-PT, PIN-PMN-PT and PMN-PT crystals are about 30-40%, 40-50% and 50-60% of their respective room temperature values.

Figure 3 shows that the d_{32}-values at −100°C of the 3 crystal systems are: 1200-1400 pC/N for both PZN-PT and PIN-PMN-PT and 1400-1600 pC/N for PMN-PT. At −150°C, the d_{32} values are: 550-750 pC/N for PZN-PT and derivatives, 750-900 pC/N for PIN-PMN-PT and 1150-1300 pC/N for PMN-PT single crystals. All the above values are significantly higher than d_{33} ≈ 350-600 pC/N for PZT piezoceramics at room temperature which drops to 25-30% of said value at cryogenic conditions.

The present results suggest that similar crystal composition and device construction to that of cost-effective stake (CE-HFS) actuators are also suitable for cryogenic applications when low out-gasing cryogenic epoxy is used in their fabrication. The cryogenic performance of a PIN-PMN-PT

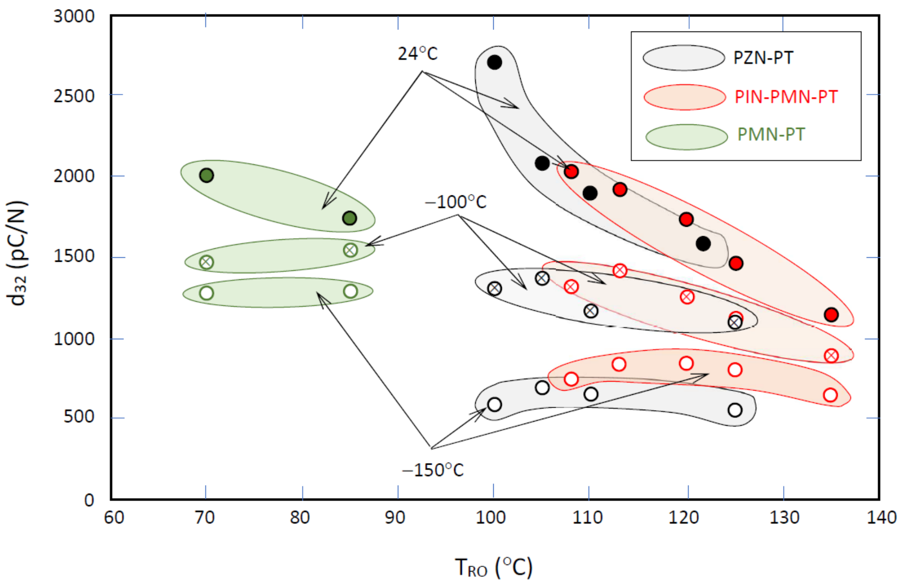

Figure 3. d_{32}-values of PZN-PT, PIN-PMN-PT and PMN-PT single crystal systems at room and two cryogenic temperatures.

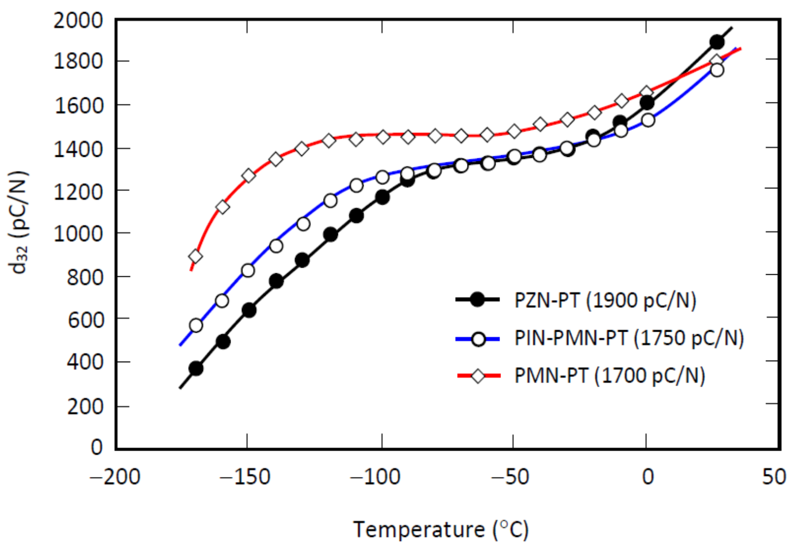

Figure 4. Representative d_{32} responses of [011]-poled PZN-PT, PIN-PMN-PT and PMN-PT single crystals as functions of temperature , all with room temperature d_{32} values of 1700-1900 pC/N.

CG-HFS prototype, 5×5×15L mm^3 in dimensions, is provided in Figure 5. This sample registers a stroke of −12.8 μm under 240V at room temperature, which decreases to −10.9 μm at 0°C, −8.4 μm at −50°C, −6.9 μm at −100°C, and further to −3.9 μm at −150°C. While the measured strokes reflect closely the variation of d_{32} with temperature shown in Figure 4, its value at −150°C is only 30-35% that at room temperature. This is possible considering the much increased elastic modulus of the polymer edge guides and the associated mechanical constraint they impose onto the crystals at cryogenic temperatures.

The transformation loads of the above-said actuator sample at different test temperatures under 240V were determined by adding weights to the actuator sample until a change in slope in the displacement curve was noted, corresponding to a change in crystal elastic stiffness and hence phase present. The obtained values are provided in Figure 5. Above said loads, local rhombohedral-to-orthorhombic phase transformation may occur in the crystals leading to deviation from linearity of the displacement response and observable strain hysteresis. The result shows that the transformation load increases substantially at cryogenic temperatures. For instance, at −50°C it is 1.5× the value at room temperature and about 2× as the temperature is lowered to −100°C and below.

Based on the measurement data, the performance of 5×5×15L CG-HFS can be deduced. The results are provided in Table 2, in which the maximum loads allowed are taken as 0.9× that of the transformation loads. Larger strokes are expected when longer lengths of single crystal active material are used. Alternatively, since both the transformation voltage and axial compressive load increase substantially at cryogenic temperatures, under low payload condition, one may decrease the crystal thickness and/or increase the applied voltage to attain higher axial displacement when such

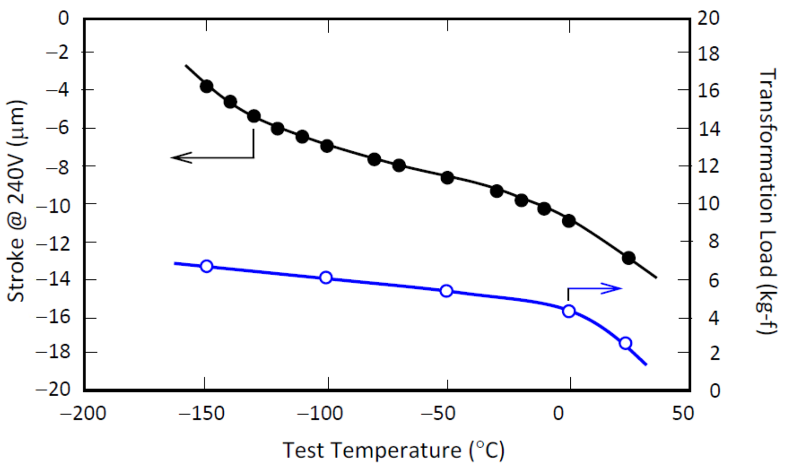

Figure 5. Stroke (@ 240V) and transformation loads (under 240V) as functions of test temperature displayed by a 5×5×15L CG-HFS stake actuator sample fabricated.

Table 2. Performance of an experimental CG-HFS sample of 5×5×15L in dimensions

Temperature (°C)	Stroke @ 240V (μm)*	Max. Load Allowed under 240V (kg-f)**
28	−12.8	2.5
0	−10.9	4.2
−50	−8.4	5.5
−100	−6.9	6.1
−150	−3.9	6.7

*Active length of crystals = 12 mm; **Taken as 0.9× transformation loads shown in Fig. 5.

is advantageous. However, this should be done with care such that there is no occurrence of local phase transformation in the single crystal active material.

Similar to CE-HFS, CG-HFS stake actuators made of PZN-PT/PIN-PMN-PT crystals can be used up to 60°C with payload. At and below said use temperature and under above-described cryogenic conditions, MMT CG-HFS stake actuator displays linear strain responses with minimum hysteresis.

The above-described CG-HFS prototype, of 5×5×15L mm in dimensions, has a capacitance of about 18 nF. This is much smaller than that exhibited by stack actuators of comparable dimensions made of either d_{33}-mode PMN-PT single crystal or PZT piezoceramics, being low to high hundreds of nF or even larger [11,15]. Since the a.c. power consumption is proportional to the product of device capacitance and square of a.c. applied voltage, taking typical applied peak voltage at 150V for stack actuators, a.c. power consumption of PZN-PT/PIN-PMN-PT single crystal stake actuators is thus only about 1/4 to 1/20 that of PZT (and PMN-PT single crystal) stack actuators despite a higher drive voltage of 240 V. MMT CG-HFS single crystal stake actuators thus not only offer reasonable stroke and payload at cryogenic temperatures but also linear, non-hysteretic strain behaviour and reduced power consumption characteristics. The economic use of single crystal volume also offers attractive cost advantage compared to PMN-PT single crystal stacks.

Figure 3 further shows that d_{32}-mode PMN-PT single crystals also make excellent cryogenic stake actuators, giving 1.5× larger stroke than that made of PZN-PT/PIN-PMN-PT crystals. Despite so, it should be noted that PMN-PT single crystals have low T_{RO} of 65-90°C. This results in their low maximum use temperature of 30-40°C for stake actuators made from them. Above said use temperature, PMN-PT single crystal stake actuators may display nonlinear and hysteretic strains due to local phase transformation occurring in the crystal, especially at sufficiently high applied voltage (of >150V) and under payload condition. Hence, the environment should be controlled to not more than 40°C or so should PMN-PT crystals be used to make cryogenic stake actuators.

4. High-Temperature Hi-Fi Stake (HT-HFS) Actuator

In the development of CE-, LS- and HL-HFS actuators, care had been exercised in the selection of crystal composition and dimensions such that the resultant stakes can achieve a reasonably high use temperature of around 60°C under payload (see Table 1 and Fig. 2). Despite so, when tested at 70°C or higher, these actuators start to display non-linear, hysteretic strains even with no payload. This holds for PMN-PT, PZN-PT and PIN-PMN-PT crystal systems of commercially available compositions. In other words, to extend the maximum use temperature to 80°C, new crystal systems of superior transformation properties, notably transformation temperature, are needed.

Shown in Table 3 are the T_{RO}, electrical and piezoelectric properties of two PIN-PZN-PT crystal compositions: one of MPB and the other of rhombohedral state. The higher T_{RO} of this crystal system is striking, being ≥150°C for PIN-PZN-PT(MPB) and ≥165°C for PIN-PZN-PT(R). Both compositions also have relatively high d_{32} values, suggesting that they are candidate materials for high-temperature Hi-Fi-Stake (HT-HFS) actuators.

Figure 6 shows the displacement responses at various test temperatures of an experimental 5×5×15L actuator sample made of d_{32}-mode crystals of PIN-PZN-PT (MPB). The displacement curves remain linear even at 80°C but hysteresis strains become apparent at the two higher temperatures, being about 3.8% and 4.7% in relative strain at 40°C and 80°C, respectively. The transformation loads at different test temperatures under 240 V were determined similarly as described above, from which the maximum loads allowed at respective temperatures were deduced (taken as 0.9× the transformation loads). The results are provided in Table 4. It is evident that PIN-PZN-PT(MPB) crystals are suitable for making HT-stake actuators. The observed hysteresis may be attributed to the higher dielectric loss of 0.005-0.008 for this crystal composition (Table 3).

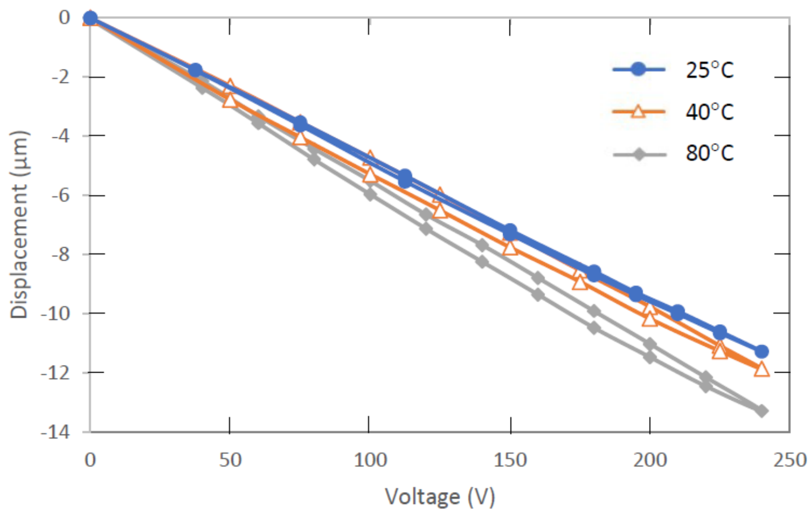

Figure 6. Displacement curves of an experimental HT-HFS actuator of 5×5×15L in dimensions at different temperatures.

Table 3. Measured properties of d_{32}-mode PIN-PZN-PT single crystals

Crystal Composition	T_{RO} (°C)	K_3^T	tanδ	d_{32} (pC/N)	k_{32}
PIN-PZN-PT(MPB)	145-160	2750-3500	0.005-0.008	–(1250-1650)	0.86-0.92
PIN-PZN-PT(R)	160-175	2000-2750	0.001-0.003	–(900-1250)	0.78-0.90

Table 4. Performance of a HT-HFS actuator sample made of PIN-PZN-PT(MPB) single crystals

Sample Type	Stroke (μm) @25°C / 240V	Max. Load Allowed under 240V (kg-f)**		
		25°C	40°C	80°C
HT-HFS (of 5x5x15L)*	11.6	4.8	3.0	1.3

*Active length of crystals = 12 mm; **Taken as 0.9× transformation loads obtained experimentally.

Our next plan is to fabricate stake actuators out of PIN-PZN-PT(R) crystals. This crystal has a smaller d-value but also lower dielectric loss (Table 3). It is thus of interest to evaluate the performance characteristics of stake actuators made of it and compare them with that made of PIN-PZN-PT(MPB) described in this work. We shall report our finding in due course.

5. Conclusions

Various versions of Hi-Fi Stake (HFS) single crystal piezoelectric actuators are described in the present work. They include: cost-effective (CE), large-stroke (LS), high-load (HL) HFS actuators. They were constructed by bonding [011]-poled d_{32}-mode lead-based relaxor-PT single crystals with polycarbonate edge guides into a square-pipe structure. For CE-, LS- and HL-HFS, careful selection of crystal composition enables the resultant actuators to display strokes of up to 50 μm @ 240 V and maximum payload of up to 14 kg-f. All can be used up to 60 °C but with reduced payloads. Within the specified conditions, they exhibit highly linear strain behaviour with negligible hysteresis.

Also discussed in detail is the development of cryogenic (CG) and high-temperature (HT) HFS actuators including crystal selection and performance evaluation. The results show that similar crystal compositions as for CE-HFS are suitable for CG-HFS except that low out-gasing cryogenic epoxy should be used in its fabrication. For enhanced stroke at cryogenic temperatures, thinner crystals may be employed and/or the drive voltage may be increased appropriately under low payload condition. Alternatively, PMN-PT crystals may be used provided that the environment is controlled to not more than 40°C or so. In contrast, new crystal compositions are needed for HT-HFS for use up to 80°C. PIN-PZN-PT crystals are candidate materials for such applications.

Acknowledgments: The authors wish to thank the staff of MMT for the technical help rendered in the present work.

Author Contributions: FCL and DHL were involved in the experimental evaluation and YX and JK in the fabrication of HFS actuators in this work. LCL is the CTO and the project manager. The paper were written jointly by FCL and LCL.

Conflicts of Interest: The authors declare no conflicts of interest.

Abbreviations

The following abbreviations are used in this manuscript:
MPB: Morphotropic phase boundary
HFS: Hi-Fi Stake
CE: Cost-effective
LS: Large stroke
HL: High load
CG: Cryogenic
HT: High temperature

References

1. Park, S.E.; and Shrout, T.R. Ultra high strain and piezoelectric behaviour in relaxor based single crystals. *J. Appl. Phys.* **1997**, *82*, 1804-1811.
2. Zhang, S.; and Li, F. High performance ferroelectric relaxor-$PbTiO_3$ single crystals: Status and perspective. *J. Appl. Phys.* **2012**, *111*, 031301.
3. Luo, J.; and Zhang, S. Advances in the growth and characterization of relaxor-PT-based ferroelectric single crystals. *Crystals* **2014**, *4*, 306-330; doi:10.3390/cryst30306.
4. Peng, J.; Lou, H.; Lin, D.; Xu, H.; He, T.; and Jin, W. Orientation dependence of transverse piezoelectric properties of $0.70Pb(Mg_{1/3}Nb_{2/3})O_3$-$0.30PbTiO_3$ single crystals. *Appl. Phys. Lett.* **2004**, *85*, 6221-6223.
5. Davis, M.; Damjanovic, D.; and Setter, N. Electric field, temperature and stress-induced phase transition in relaxor ferrorlectric single crystals. *Phys. Rev. B* **2006**, *73*, 014115; doi:10.1103/PhysRevB.73.014115.
6. Feng, Z.; Li, H.; and Luo, H. High electric-field-induced strain behaviour of single crystal $Pb(Mg_{1/3}Nb_{2/3})O_3$ -$PbTiO_3$ multilayer piezoelectric actuators. *J. Electron. Mater*. **2005**, *34*, 1035-1039.
7. Jiang, X.; Rehrig, P.W.; Luo, J.; Hackenberger, W.S.; Zhang, S.; and Shrout, T.R. Low voltage single crystal actuators. *Proc. SPIE* **2006**, *6170*, 61700G.
8. Huang, Y.; Xia, Y.X.; Lin, D.H.; Yao, K.; and Lim, L.C. Large stroke high fidelity PZN-PT single crystal 'Stake' actuator. *IEEE Trans. Ultrason. Ferroelectr. Freq. Control* **2017**, *64*, 1617-1624.
9. Huang, Y.; Zhang, Z.; Wang, P.; Xia, Y.X.; Lin, D.H.; Yao, K.; and Lim, L.C. Hi-Fi Stake piezo single crystal actuator. *Actuators* **2018**, *7*, 60; doi: 10.3390 / act7030060.
10. http://www.microfine-piezo.com/assets/pdf/HIFI-Actuator.pdf
11. Wise, S.A. Characterisation of multilayer piezoelectric actuators for use in active isolation mounts. *NASA Tech Memo*. 4742, 1997.
12. NASA JWST Cryogenic Actuator Activities, http//ngst.gsfc.nasa.gov/hardware/text/actuatoractivities.html.

13. Paik, D.S.; Park, S.E.; Heckenberger, W.S.; and Shrout, T.R. Dielectric and piezoelectric properties of perovskite materials at cryogenic temperatures. *J. Mater. Sci*, **1998**, *34*, 469-473.
14. Jiang, X.N.; Rehrig, P.W.; Hackenberger, W.S.; Smith, E.; Dong, S.; Viehland, D.; Moore, J.; and Patrick, B. Advanced piezoelectric single crystal based actuators. *Proc. SPIE* **2005**, *5761*, 253-262.
15. Nature>>Universe>>Is It Hot Or Cold At The International Space Station?